J Nanopart Res (2009) 11:1117–1127
DOI 10.1007/s11051-008-9505-x

RESEARCH PAPER

Effect of voids and pressure on melting of nano-particulate and bulk aluminum

Puneesh Puri · Vigor Yang

Received: 10 March 2008 / Accepted: 29 August 2008 / Published online: 11 October 2008

Abstract Molecular dynamics simulations are performed using isobaric–isoenthalpic (NPH) ensembles to study the effect of internal defects in the form of voids on the melting of bulk and nano-particulate aluminum in the size range of 2–9 nm. The main objectives are to determine the critical interfacial area required to overcome the free energy barrier for the thermodynamic phase transition, and to explore the underlying mechanisms for defect-nucleated melting. The inter-atomic interactions are captured using the Glue potential, which has been validated against the melting temperature and elastic constants for bulk aluminum. A combination of structural and thermodynamic parameters, such as the potential energy, Lindemann index, translational-order parameter, and radial-distribution functions, are employed to characterize the melting process. The study considers a variety of void shapes and sizes, and results are compared with perfect crystals. For nano aluminum particles smaller than 9 nm, the melting temperature is size dependent. The presence of voids does not impact the melting properties due to the dominancy of nucleation at the surface, unless the void size exceeds a critical value beyond which lattice collapse occurs. The critical void size depends on the particle dimension. The effect of pressure on the particulate melting is found to be insignificant in the range of 1–300 atm. The melting behavior of bulk aluminum is also examined as a benchmark. The critical interfacial area required for the solid–liquid phase transition is obtained as a function of the number of atoms considered in the simulation. Imperfections such as voids reduce the melting point. The ratio between the structural and thermodynamic melting points is 1.32. This value is comparable to the ratio of 1.23 for metals like copper.

Keywords Aluminum · Voids · Nanoparticles · Melting · Molecular dynamics · Modeling and simulation

Abbreviations

Al	Aluminum
f	Ratio of structural to thermodynamic melting point
r_{ij}	Distance between two atoms
U	Potential energy
φ	Potential function
ρ	Density function

Introduction

Nano-sized aluminum and other metallic particles have been extensively used in many propulsion and energy-conversion applications due to their unusual

P. Puri (✉) · V. Yang
The Pennsylvania State University, University Park, PA 16802, USA
e-mail: pxp916@psu.edu

V. Yang
e-mail: vigor@psu.edu

energetic properties, such as increased catalytic activity and higher reactivity (Ilyin et al. 2001; Kwon et al. 2003). The excess energy of surface atoms and reduced activation energies for chemical reactions contribute to these extraordinary chemical characteristics (Pivkina et al. 2004). Much effort has been applied to characterize nano-material properties. There, however, still exist inconsistencies and uncertainties in various theories concerning the particle behavior at nano scales (Rai et al. 2004; Rozenband and Vaganova 1992; Dreizin 2003; Trunov et al. 2006). Fundamental research based on well-calibrated techniques appears to be imperative, in order to achieve improved understanding of the effect of particle size and other parameters like internal defects on material properties.

From a structural point of view, voids have been the subject of research for both the bulk and particulate phases. Allard et al. (1994) reconstructed the images of 5–15 nm palladium particles from electron holograms using a field-emission-transmission electron microscope, and reported for the first time the existence of internal voids in metallic particles. Shimomura and Moritaki (1981) discussed the formation of voids in pure aluminum quenched in hydrogen gas. The number density of voids was found to be proportional to the square root of the partial pressure of hydrogen in the gas. Nano-void deformation in aluminum subject to cyclic shear deformations was examined by Marian et al. (2005) and the growth of these voids under hydrostatic tensions was examined by Marian et al. (2004). Hyuk et al. (2005) developed techniques for preparing colloidal particles with hollow interiors. In addition, considerable progress has been recently made in molecular self assembly and supra molecular control for synthesizing and assembling nano-structured energetic materials (Yetter 2008). Aluminum nanoparticles manufactured as a result of these efforts may likely contain internal voids of some sort.

The term melting point has been used in the literature with different definitions. *Experimental melting point* is the temperature for phase transition as observed in an experimental set up. *Thermodynamic* and *structural melting points* are terms used in theoretical and numerical studies. The former, T_m, ideally should be identical to the experimental melting point for a real solid. It is based on the coexistence of the solid and liquid phases, and theoretically is the temperature at which the solid and liquid Gibbs free energies are equal. Since calculation of free energies is a non-trivial task, in most molecular dynamics studies, the bulk is simulated using periodic boundary conditions without any defects. Such a numerical framework produces structural melting, T_s. The absence of any nucleation sites in a perfect crystal leads to heating the substance beyond T_m, a phenomenon known as superheating. Structural melting refers to the limit beyond which there is general collapse of lattice structure. Results obtained from a numerical simulation correspond to either structural or thermodynamic melting, depending on the properties of the initial crystal. The theories regarding vibrational instability, lattice shear instability, and catastrophic generation of dislocations are associated with structural melting.

Deliberately introducing clusters of vacancy defects to avoid superheating in a perfect crystal is referred as defect-nucleated melting. The concept was introduced and reported in the numerical studies by Lutsko et al. (1989) and Phillpot et al. (1989). These studies highlighted the fact that the nucleation of the liquid phase at the defect is the dominant initiation mechanism of melting, and hence the melting of an ideal crystal with periodic boundary conditions takes place at a temperature higher than the experimental melting point. Phillpot et al. (1989) investigated the melting characteristics of silicon in the presence of a grain boundary and a free surface (110) using molecular dynamics simulations associated with the Stillinger–Weber potential. Lutsko et al. (1989) simulated the high-temperature behavior of a grain boundary, free surface and a planar array of voids on (001) plane of copper using the embedded-atom-method potential. The investigation found structural and thermodynamic melting points of 1450 and 1171 K, respectively, for copper. Recently, the concept of defect-nucleated melting has been implemented by Solca et al. (1997, 1998) to determine the theoretical melting curves of argon and neon, as a function of pressure using isobaric–isoenthalpic (NPH) molecular dynamics and Lennard–Jones potentials. The structural melting points for an ideal crystal were found to be 20% higher than the thermodynamic melting points for lattices with a defect in the form of a void. The work of Lutsko et al. (1989) shows that there exists a constant ratio between the structural and

thermodynamic melting points ($f = T_s/T_m$). For copper and argon, the ratios are 1.234 and 1.176, respectively (Lutsko et al. 1989; Solca et al. 1997). Agarwal et al. (2003) simulated defect-nucleated melting of argon over a broader range of pressures of 0.094–531.6 kbar. The melting point was found to be independent of the shape and location of the void.

Experimental studies have suggested that small atomic clusters exhibit characteristics different from those of a bulk substance. A decrease of the melting point by 30% has been measured in metallic clusters of diameters of 20–30 Å (Buffat and Borel 1976). A modification of surface conditions can depress the melting point or substantially superheat the solid. An ideal crystal melts at a temperature higher than the experimental or thermodynamic melting point, and imperfections such as voids reduce the melting point. The extent to which these imperfections affect the melting point, however, is very subjective and varies with substance. As the presence of a surface acts as a nucleation site for melting, an alteration in the surface properties can have a major impact on the melting temperature and related phenomena for the substance.

In our earlier work based on molecular dynamics simulations, the effects of particle size and surface charge development on the melting of particulate aluminum were investigated in the range of 2–9 nm (Puri and Yang 2007). The work involved nano-sized aluminum particles in the range of 2–9 nm. Results indicated that as the particle size decreases below a critical value (8 nm), owing to the increase in the surface-to-volume ratio, the melting temperature becomes a size-dependant property and decreases monotonically with decreasing diameter, from a bulk value of 937 K at $\sim$8 nm to 473 K at 2 nm (Puri and Yang 2007). The finding is consistent with those from other experimental and numerical studies (Alavi and Thompson 2006; Wronski 1967; Eckert et al. 1993; Bucher et al. 2000). As an extension of our previous work, the current research explores the effect of pressure and defects in the form of voids on the melting characteristics of nano-particulate aluminum in the range of 2–9 nm where bulk properties break down.

The present work involves MD simulations using an NPH ensemble. The Glue potential is selected to treat the inter-atomic interactions, because of its ability to capture the size dependence of thermodynamic properties for particulate aluminum (Puri and Yang 2007). A combination of structural and thermodynamic parameters, including the potential energy, Lindemann index, translational-order parameter, and radial-distribution functions, are used to characterize the melting process. For the particulate phase, spherical nanoparticles up to 9.0 nm are considered. Voids of different shapes and sizes are taken into account, and results are compared with perfect particles having no defects. The underlying mechanisms of the entire melting process are examined using snapshots of the time evolution of atomic positions and density contours. For the bulk phase, crystals composed of 864 and 2048 atoms are considered. The structural melting point, T_s, for an ideal crystal is found to be 32% higher than the thermodynamic melting point, T_m, for lattices with a defect.

Theoretical and computational framework

The basis of the present work is the general theoretical and computational framework established in our previous MD study of aluminum melting (Puri and Yang 2007). In short, the NPH ensemble is employed to model the melting of the bulk and nano-particulate aluminum. A system of N atoms is coupled to an external source by introducing additional variables into the Lagrangian using volume as an extra degree of freedom through mechanical coupling (Anderson 1980). The equations of motion are numerically integrated using a fifth-order predictor–corrector algorithm (Allen and Tildesley 1989). The time step is chosen to be 1 femto-second, considering that the time scale for vibration of atoms is of the same order. Annealing is achieved using velocity scaling, and the temperature of the nanoparticle is increased at a rate of 0.01 K/time step. A parametric study was performed on a bulk FCC crystal consisting of 2048 atoms with different temperature rises of 1, 0.1, 0.01, and 0.001 K/femto-second for each time step. A rate lower than 0.01 K/step increases the total computational time, and a higher rate gives insufficient time for particles to equilibrate at each step. An optimum rate of 0.01 K/step also helps predict the melting point accurately, because it produces better resolution in the variations of thermodynamic and structural properties.

The macroscopic thermodynamic properties of the system are derived from the instantaneous values using the equation of state and statistical mechanics. A combination of structural and thermodynamic parameters, including the potential energy, Lindemann index (Zhou et al. 2002), translational-order parameter (Gezelter et al. 1997), and radial-distribution functions, are used to characterize the melting process. The general computational framework can handle micro-canonical (NVE), NPH, and isobaric–isothermal (NPT) ensembles using both the Verlet and predictor–corrector algorithms. These algorithms have been parallelized using the atomic decomposition method (Plimpton 1995). A separate post-processing code has also been developed to superimpose the grid on the geometry under consideration, and to analyze the results using the contours of various thermodynamic properties. The code has the capability of handling multi-atom simulations, and can treat liquid and solid phases.

In our previous MD study, five different potential functions for aluminum (i.e., the Lennard–Jones, Glue, Embedded Atom, Streitz–Mintmire, and Sutton–Chen potentials) were implemented and the results were compared using the size dependence of the melting phenomenon as a benchmark (Puri and Yang 2007). Two-body potentials like the Lennard–Jones potential failed to capture the thermodynamic melting phenomenon. The Sutton–Chen potential, fitted to match structural properties, also failed to capture the size dependence of the particle melting point. Many body potentials like the Glue and Streitz–Mintmire potentials resulted in accurate melting temperature as a function of particle size. The latter is computationally more expensive. For calculations involving perfect aluminum without any charges, this potential involves unnecessary computational overheard in terms of charge calculations. The Glue potential is thus selected for the present study. It is defined by a pair potential $\varphi(r)$, an atomic density function $\rho(r)$, and a Glue function $U(\rho)$, and can be expressed as (Ercolessi and Adams 1994)

$$V_{\text{glue}} = \frac{1}{2}\sum_{i,j}\varphi(r_{ij}) + \sum_{i} U\left(\sum_{j}\rho(r_{ij})\right)$$

The NVE and NPH algorithms developed in the present study have been validated against argon in different (i.e., solid, liquid, and vapor) phases and its thermodynamic transition from the solid to the liquid phase, because of the availability of extensive and reliable experimental and numerical data (Solca et al. 1997, 1998). Details on the computational framework, comparison of different potentials and validation studies for the MD code are given in Puri and Yang (2007).

Results and discussion

The general framework outlined in Theoretical and computational framework section was first applied to study the melting of bulk aluminum with and without defects. The simulations were carried out by arranging atoms in a FCC lattice structure and evolving the system with periodic boundary conditions. Figure 1 shows the variations of thermo-mechanical properties with increasing temperature for a perfect crystal of 864 atoms in a vacuum. Homogeneous melting due to lattice instability was observed at a temperature of 1244 K, as evidenced by abrupt changes in the potential energy, atomic density, Lindemann index, translational order parameter, and radial distribution function. During melting the distance between atoms increases, and hence the potential energy increases and the atomic density decreases sharply. The Lindemann index measures the vibrational motion of particles. It is calculated as a function of the distance between the atoms and increases as a result of phase change. The translational-order parameter is indicative of the ordered structure in a given phase. It has a value of approximately unity for a solid state, and drops to nearly zero for a liquid state.

This phenomenon is commonly referred to as structural melting, and the associated transition temperature is greater than the thermodynamic melting point (940 K) by 32%.

To obtain the ratio between the structural and thermodynamic melting points, bulk crystals with different void sizes in the range of 0.19–4.0 nm^3 were considered, as shown in Fig. 2. The procedure followed the same approach adopted in previous studies (Lutsko et al. 1989; Phillpot et al. 1989; Solca et al. 1998; Solca et al. 1997; Agarwal et al. 2003). The influences of void shape and location were also treated. For example, a void of 1.05 nm^3 can be implemented by creating either a $4 \times 2 \times 2$ nm^3 or a $4 \times 4 \times 1$ nm^3 void geometry, through the removal

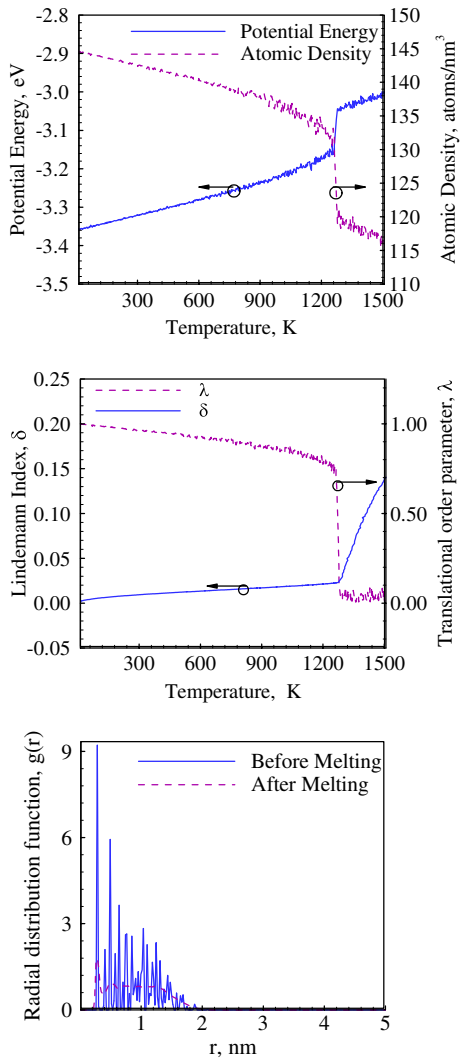

Fig. 1 Variations of structural and thermodynamic properties during melting of bulk aluminum; perfect crystal of 864 atoms without defects

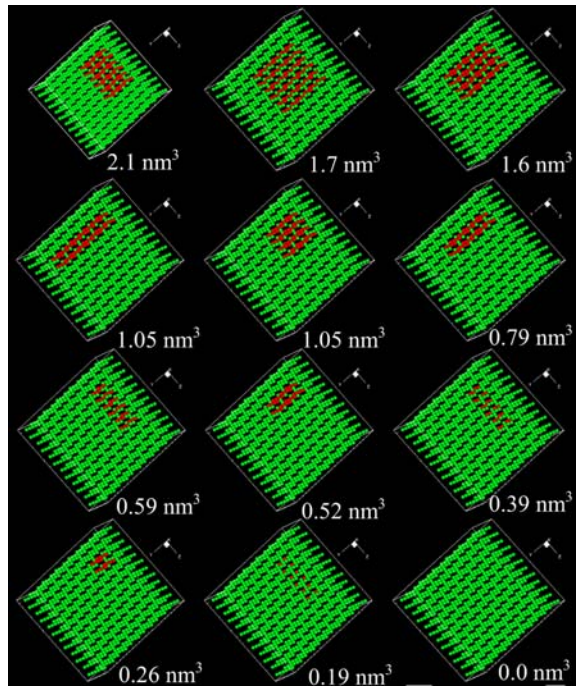

Fig. 2 Different void geometries considered for bulk aluminum with 864 atoms

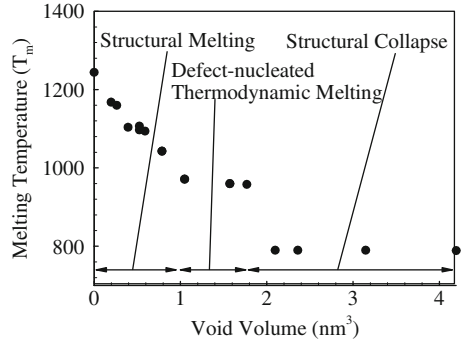

Fig. 3 Effect of void size on melting of bulk aluminum with 864 atoms

of 64 atoms from a crystal of 864 atoms. Voids provide a nucleation site for simulating thermodynamic melting. There, however, exists a range of critical void size for thermodynamic melting. A very small void size is insufficient for nucleation of the liquid phase, and a void size larger than the critical value can cause collapse of the crystal. As compared to 1244 K for a perfect crystal, the melting point for a crystal with voids initially decreases with void size, and then plateaus close to the thermodynamic melting point of aluminum, as seen in Fig. 3. The situation is consistent with observations made in previous studies on argon and copper (Lutsko et al. 1989; Solca et al. 1997). When the void size exceeds 1.7 nm^3, the crystal collapses suddenly, and the phenomenon of phase change cannot be simulated.

The melting temperature is a function only of the volume of the void, not its shape. For a volume of 1.05 nm^3, the two geometries shown in Fig. 2 produce exactly the same melting point. When the void size falls in the range of 1.0–1.7 nm^3, the void only provides a nucleation site and leads to the same

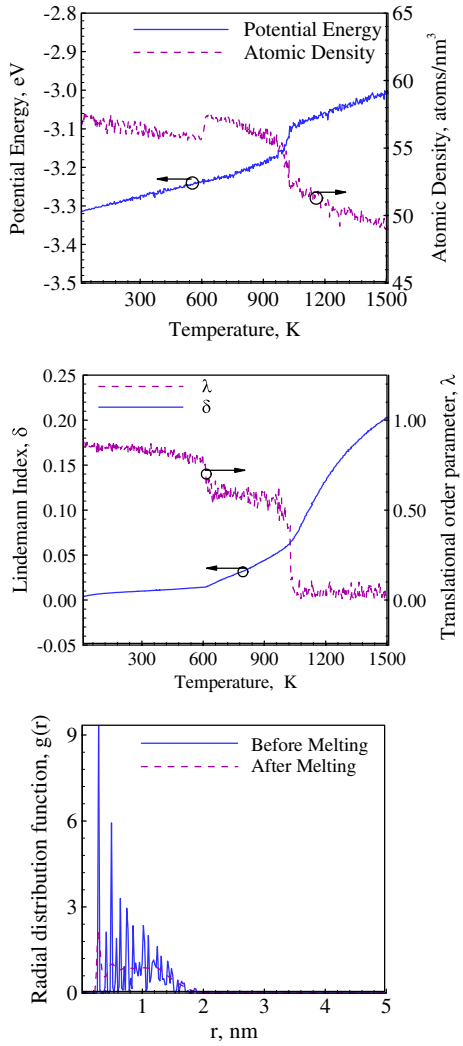

Fig. 4 Variations of structural and thermodynamic properties during melting of bulk aluminum; crystal of 864 atoms with 1.05 nm^3 void

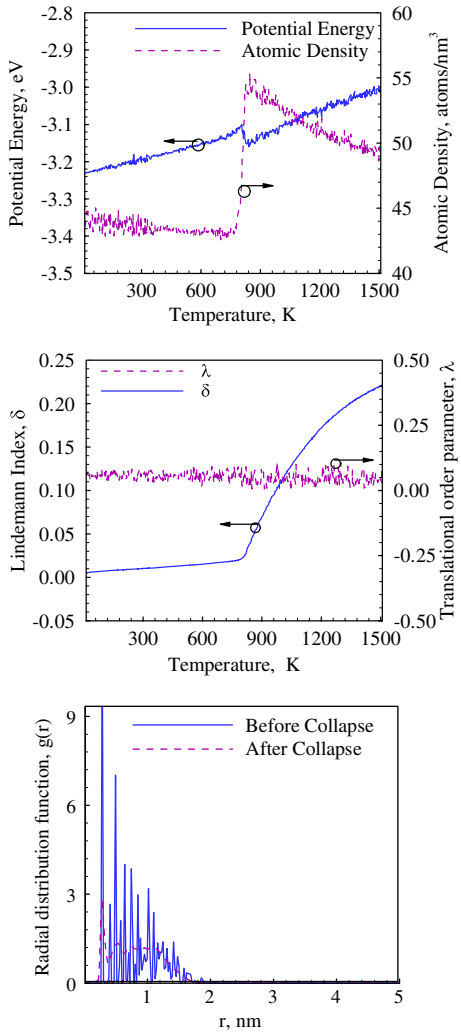

Fig. 5 Variations of structural and thermodynamic properties of bulk aluminum showing lattice collapse; crystal of 864 atoms with 4.0 nm^3 void

temperature for the phase change, i.e., the thermodynamic melting point, irrespective of the shape of the void. From all these cases, the ratio of 1.32 between the structural and thermodynamic melting points was consistently obtained.

Figure 4 shows the case of thermodynamic melting for a 1.05 nm^3 void. The variations of properties are not as steep as the structural melting because of the nucleation at the void. The situation with a large void size of 4.0 nm^3 is shown in Fig. 5, for which the crystal collapses. The potential energy decreases, but the atomic density increases. The trend is opposite to that observed during melting. The whole phenomenon occurs at a temperature (800 K) much lower than the thermodynamic melting point (940 K), indicating the collapse of the crystal and no phase change.

Figure 6 shows the temporal evolution of atomic positions, illustrating the difference among the structural melting, thermodynamic melting, and lattice collapse of the crystal. In the case of structural melting, the phase transition is abrupt and homogeneous, as seen in Fig. 6a. The crystal has solid structure up to 124.2 ps, and a phase change occurs suddenly at 126.9 ps, due to vibrational instability without any nucleation. In the case of thermodynamic melting, however, the nucleation starts near the void,

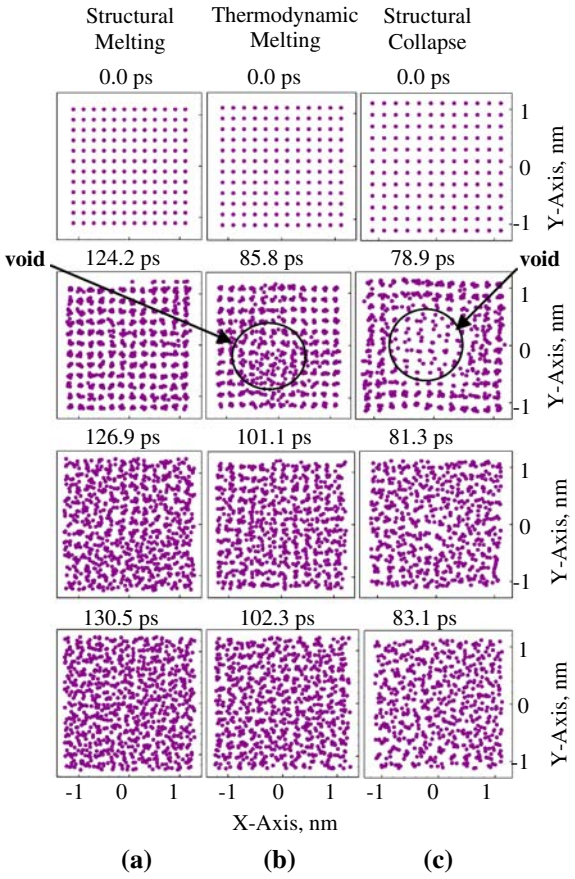

Fig. 6 Temporal evolution of atomic positions, showing mechanisms of melting and structural collapse for bulk aluminum with 864 atoms: (**a**) without defect, (**b**) with a void size of 1.05 nm^3, and (**c**) with a large void size of 4 nm^3

as indicated by the local concentration of atoms around the void, and proceeds to the rest of the crystal. Figure 6b shows thermodynamic melting with a void size of 1.05 nm^3. The nucleation starts near the void at 85.8 ps, and the whole crystal melts by 102.3 ps. If the void size exceeds its critical value, the whole crystal collapses and cannot be put in the category of either thermodynamic or structural melting. The breakdown of the structure with a void of 4 nm^3 is evidenced in Fig. 6c, and is comparatively different from the mechanism of melting. At 78.9 ps, when the temperature of the crystal is around 790 K, the atoms close to the void leave their positions and fill up the void space. No phase change is observed in this case.

To study the effect of the number of atoms in bulk aluminum on defect-nucleated melting, a similar analysis was performed for a crystal with 2048 atoms.

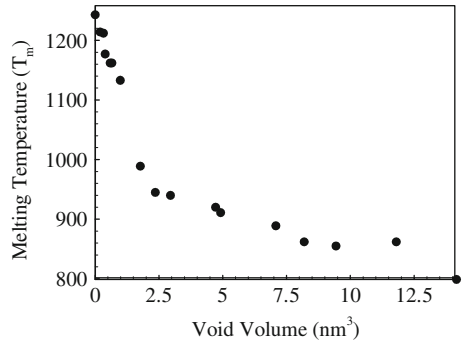

Fig. 7 Effect of void size on melting of bulk aluminum with 2,048 atoms

The structural and thermodynamic melting points (plateau region) are the same as those for 864 atoms, i.e., 1244 and 940 K, respectively. Figure 7 shows the variation of the melting point as a function of void size for bulk aluminum with 2048 atoms. The structural melting point for a perfect crystal is observed at 1244 K, and the melting point decreases as the void size increases, showing a trend identical to that of bulk with 864 atoms.

The range of the void size for defect-nucleated melting increases as the number of atoms considered to represent the bulk phase increases. Figure 8 shows the variation of the critical void size for the lattice collapse as a function of bulk volume. For 2048 atoms, a void size on the order of 2–5 nm^3 results in thermodynamic melting, as compared to 1–1.7 nm^3 for 864 atoms. From the study of perfect crystals, it can be concluded that the ratio between the structural and thermodynamic melting points ($f = T_s/T_m$) for aluminum is 1.32, close to the ratio of 1.234 for

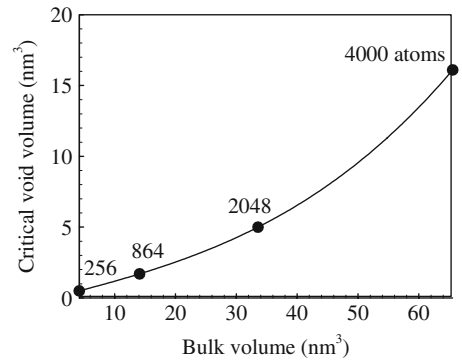

Fig. 8 Variation of critical void size for lattice collapse as a function of bulk aluminum volume

metals like copper. Copper is known to have stronger cohesive forces than aluminum, and hence should have a higher structural melting point than aluminum. The thermodynamic melting point of copper is 1357 K, and the corresponding structural melting point is 1674 K, while that for aluminum is 1244 K.

After establishing the benchmark result for bulk aluminum, effort was applied to explore the melting of nano particulates in the range of 2.0–9.0 nm. The effect of voids with different geometries and sizes were considered. Results were compared for particles with and without voids. Figure 9 shows some of the defect configurations treated for a 5.5 nm nanoparticle (5,072 atoms). The influence of void size up to 14.1 nm^3 on the melting temperature is given in Fig. 10. The melting temperature remains constant at 912 K (Puri and Yang 2007) for small voids up to 1 nm^3. Since the surface is already available for nucleation, the presence of a small void just acts as another nucleation site and exerts little influence on the thermodynamic phase change. The melting point, starts dropping as the void volume increases beyond 1 nm^3, due to the increase in forces causing the structural instability. As the void size exceeds 8 nm^3, the particle is unable to hold these forces associated with the introduction of the void, and the crystal collapses abruptly at 700 K for a 10-nm^3 void.

The melting phenomenon is also examined through the evolution of atomic positions and density contours in Figs. 11 and 12, respectively. In Fig. 12a, the nucleation process commences at 97.2 ps and is completed by 108.9 ps for a perfect nanoparticle. In the case with a void size of 0.98 nm^3, the nucleation starts simultaneously at the surface and void at 92.1 ps. The phase change spreads to the rest of the particle until melting occurs at 107.1 ps, as evidenced

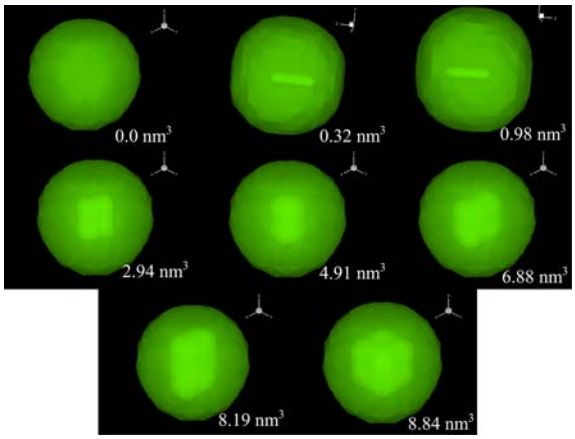

Fig. 9 Different void geometries considered for a spherical 5.5-nm aluminum particle

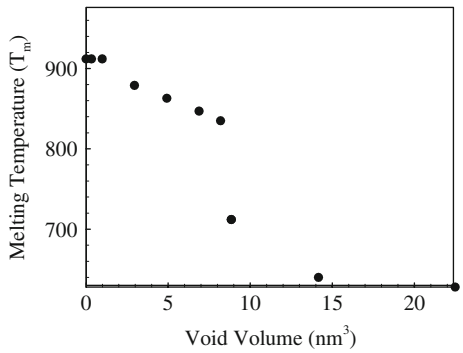

Fig. 10 Effect of void size on melting for a spherical 5.5-nm aluminum particle

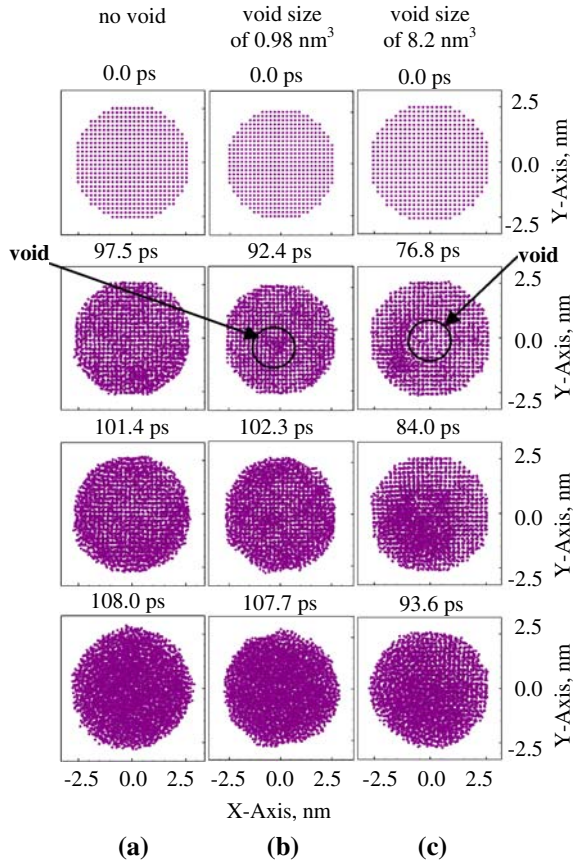

Fig. 11 Time evolution of atomic positions, showing mechanism of melting for a 5.5-nm nanoparticle: (**a**) without defect, (**b**) with a void size of 0.98 nm^3, (**c**) with a large void size of 8.2 nm^3

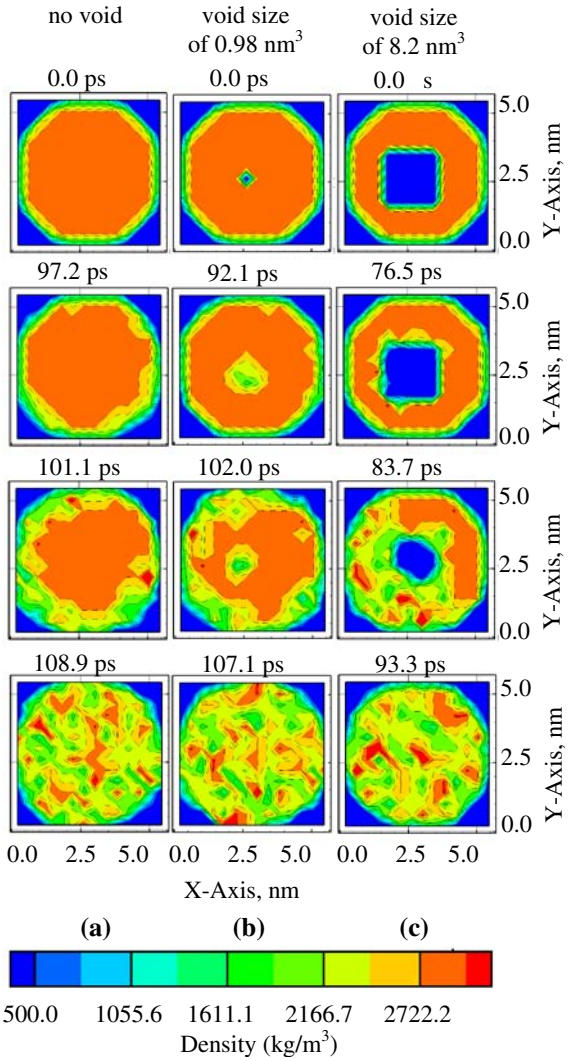

Fig. 12 Time evolution of density contours, showing mechanism of melting for a 5.5-nm nanoparticle: (**a**) without defect, (**b**) with a void size of 0.98 nm^3, (**c**) with a large void size of 8.2 nm^3

in Fig. 12b. The void size of 8.2 nm^3 shown in Fig. 12c is too big for the particle to retain its structural stability, and the particle starts collapsing at 76.5 ps. The above analysis was conducted in a vacuum. The effect of pressure was investigated at 1, 5, 10, 50, 100, and 300 atm. The influence was found to be negligible, and the same melting temperature was observed for all the pressures considered. The effect of pressure on bulk aluminum has been explored in the literature based on the Lindemann law and Chopelas–Boehler approximation and was found to be effective only for pressures of the order

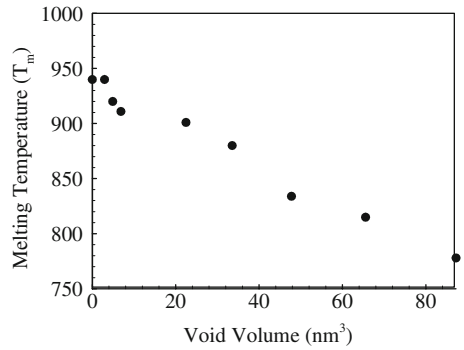

Fig. 13 Effect of void size on melting of a spherical 8.5-nm aluminum nanoparticle

of GPa (Zou and Chen 2005). The current study was performed in the range 1–300 atm, which is suitable for combustion applications. The conclusion about pressure independence is thus consistent with other theoretical studies.

A similar phenomenon was observed for a 8.5-nm particle, as shown in Fig. 13. Thermodynamic melting occurs at 940 K, which is in agreement with the previous result (Puri and Yang 2007). There is no variation in the melting point by introduction of a void up to 5 nm^3. The deviation from the thermodynamic melting point then occurs due to the effect of nucleation near the void. As the void size increases, the lattice stability decreases, further lowering the melting point. The lattice structure of the particle collapses when the void size becomes around 20 nm^3. The melting mechanism can also be explored by the temporal evolution of atomic positions and density contours shown in Figs. 14 and 15, respectively. For a perfect particle, the phase change proceeds from the surface to the interior, as evidenced in Figs. 14a and 15a. For the void size of 5 nm^3, nucleation starts at both the void and surface at 92 ps, as shown in Figs. 14b and 15b. For a large void size of 20 nm^3 exceeding the critical value, lattice collapse occurs directly at 57.4 ps, and no phase change is observed, as indicated in Figs. 14c and 15c.

Summary and conclusions

The effect of defects in the form of voids on the melting of bulk aluminum and aluminum nano-particulates in the size range of 2–9 nm has been studied using NPH

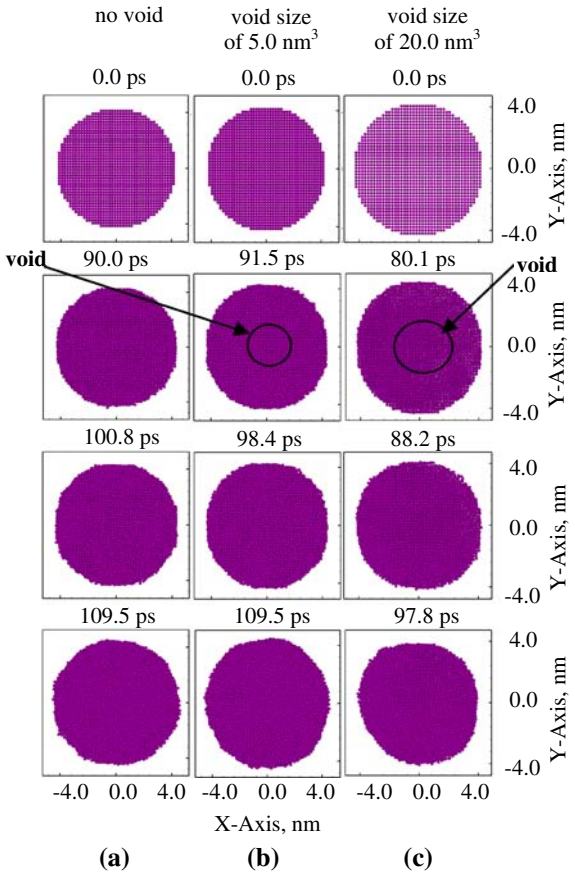

Fig. 14 Time evolution of atomic positions, showing mechanism of melting for a 8.5-nm nanoparticle: (**a**) without defect, (**b**) with a void size of 5.0 nm^3, (**c**) with a large void size of 20.0 nm^3

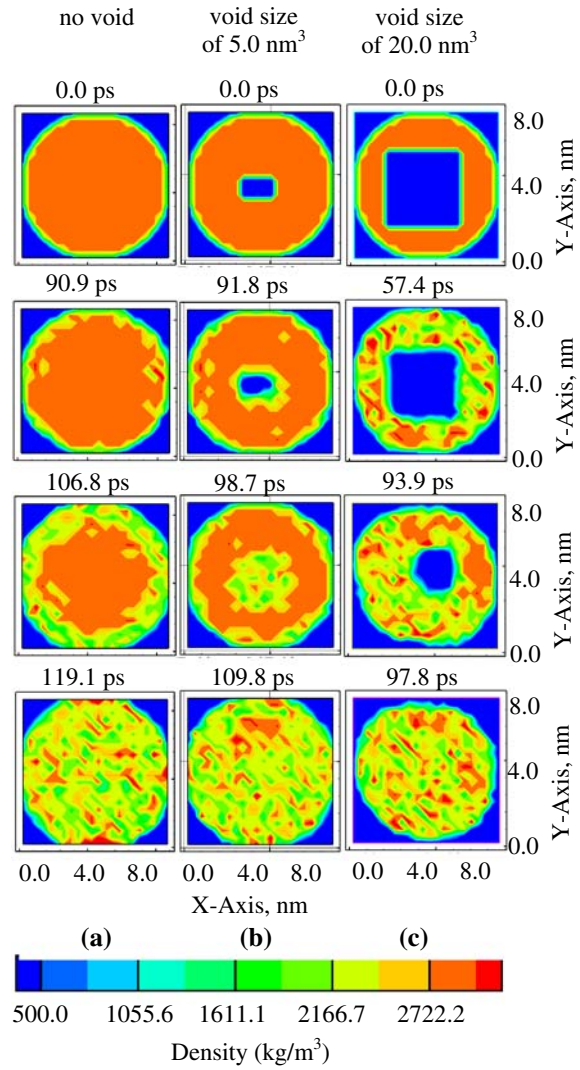

Fig. 15 Time evolution of density contours, showing mechanism of melting for a 8.5-nm nanoparticle (**a**) without defect, (**b**) with a void size of 5.0 nm^3, (**c**) with a large void size of 20.0 nm^3

ensembles. A variety of void shapes and sizes were treated, and results were compared with perfect materials. Detailed mechanisms dictating the melting phenomenon were explored. For nano particles, nucleation occurs simultaneously at both the surface and void. Void becomes effective only if its size exceeds a critical value, which increases with increasing size of the particle. For 5.5 and 8.5 nm particles, the critical void sizes are 1 and 5 nm^3, respectively. The effect of pressure on the melting of nano-particulate aluminum was found to be insignificant in the range of 1–300 atm. For bulk aluminum, the structural melting of aluminum takes place at a temperature of 1244 K. The ratio between the structural and thermodynamic melting points was found to be 1.32, independent of the void shape and size. This ratio was comparable to the result obtained for other metals like copper.

Acknowledgments This work was sponsored by the U.S. Army Research Office under the Multi-University Research Initiative under Contract No. W911NF-04-1-0178. The support and encouragement provided by Dr. Ralph Anthenien is gratefully acknowledged.

References

Agarwal PM, Rice BM, Thompson DL (2003) Molecular dynamics study of effects of voids and pressure in defect nucleated melting simulations. J Chem Phys 118:9680–9688. doi:10.1063/1.1570815

Alavi S, Thompson DL (2006) Molecular dynamics simulations of melting of aluminum nanoparticles. J Phys Chem A 110:1518–1523. doi:10.1021/jp053318s

Allard LF, Voelkl E, Kalakkad DS, Datye AK (1994) Electron holography reveals the internal structure of palladium nano-particles. J Mater Sci 29:5612–5614. doi:10.1007/BF00349955

Allen MP, Tildesley DJ (1989) Computer simulation of liquids. Oxford Science, Oxford

Anderson HC (1980) Molecular dynamics simulations at constant pressure and/or temperature. J Chem Phys 72:2384. doi:10.1063/1.439486

Bucher P, Ernst L, Dryer FL, Yetter RA, Parr TP, Hanson DM (2000) Detailed studies on the flame structure of aluminum particle combustion. In: Yang V, Brill TB, Ren WZ (eds) Solid propellant chemistry, combustion and motor interior ballistics, vol 185. Progress in Astronautics and Aeronautics AIAA, Reston, VA, pp 689–722

Buffat P, Borel JP (1976) Size effect of the melting temperature of gold particles. Phys Rev A 13:2287–2298. doi:10.1103/PhysRevA.13.2287

Dreizin EL (2003) Effect of phase changes on metal particle combustion processes. Combust Explos Shock Waves 39:681–693. doi:10.1023/B:CESW.0000007682.37878.65

Eckert J, Holzer JC, Ahn CC, Fu Z, Johnson WL (1993) Melting behavior of nanocrystalline aluminum powders. Nanostruct Mater 2:407–413. doi:10.1016/0965-9773(93)90183-C

Ercolessi F, Adams JB (1994) Interatomic potentials from first principles calculations: the force-matching method. Europhys Lett 26:583–588. doi:10.1209/0295-5075/26/8/005

Gezelter JD, Rabani E, Berne BJ (1997) Can imaginary instantaneous normal mode frequencies predict barriers to self-diffusion? J Chem Phys 107:4618–4627. doi:10.1063/1.474822

Hyuk I, Jeong U, Xia Y (2005) Polymer hollow particles with controllable holes in their surfaces. Nat Mater 4:671–675. doi:10.1038/nmat1448

Ilyin AP, Gromov AA, Vereshchagin VI, Popenko EM, Surgin VA, Lehn H (2001) Combustion of agglomerated ultrafine aluminum powders in air. Combust Explos Shock Waves 37:664–669. doi:10.1023/A:1012928130644

Kwon YS, Gromov AA, Ilyin AP, Popenko EM, Rim GH (2003) The mechanism of combustion of superfine aluminum powders. Combust Flame 133:385–391. doi:10.1016/S0010-2180(03)00024-5

Lutsko JF, Wolf D, Phillpot SR, Yip S (1989) Molecular dynamics study of lattice-defect nucleated melting in metals using an embedded-atom-method potential. Phys Rev B 40:2841–2855. doi:10.1103/PhysRevB.40.2841

Marian J, Knap J, Ortiz M (2004) Nanovoid cavitation by dislocation emission in aluminum. Phys Rev Lett 93:165503

Marian J, Knap J, Ortiz M (2005) Nanovoid deformation in aluminum under simple shear. Acta Mater 53:2893–2900. doi:10.1016/j.actamat.2005.02.046

Phillpot SR, Lutsko JF, Wolf D, Yip S (1989) Molecular dynamics study of lattice-defect-nucleated melting in silicon. Phys Rev B 40:2831–2840. doi:10.1103/PhysRevB.40.2831

Pivkina A, Ulyanova P, Frolov Y, Zavyalov S, Schoonman J (2004) Nanomaterials for heterogeneous combustion. Propellants Explos Pyrotech 29:39–48. doi:10.1002/prep.200400025

Plimpton S (1995) Fast parallel algorithms for short range molecular dynamics. J Comput Phys 117:1–19. doi:10.1006/jcph.1995.1039

Puri P, Yang V (2007) Effect of particle size on melting of aluminum at nano scales. J Phys Chem C 111:11776–11783. doi:10.1021/jp0724774

Rai A, Lee D, Park K, Zachariah MR (2004) Importance of phase change of aluminum in oxidation of aluminum nanoparticles. J Phys Chem B 108:14793–14795. doi:10.1021/jp0373402

Rozenband VI, Vaganova NI (1992) A strength model of heterogeneous ignition of metal particles. Combust Flame 88:113–118. doi:10.1016/0010-2180(92)90011-D

Shimomura Y, Moritaki Y (1981) On the important effect of water vapor in the atmosphere on void formation in quenched pure aluminum. Jpn J Appl Phys 20:2287–2293

Solca J, Anthony JD, Steinebrunner G, Kirchner B, Huber H (1997) Melting curves for argon calculated from pure theory. J Chem Phys 224:253–261. doi:10.1016/S0301-0104(97)00317-0

Solca J, Dyson AJ, Steinebrunner G, Kirchner B, Huber H (1998) Melting curves for neon calculated from pure theory. J Chem Phys 108:4107–4111. doi:10.1063/1.475808

Trunov MA, Schoenitz M, Dreizin EL (2006) Effect of polymorphic phase transformations in alumina layer on ignition of aluminium particles. Combust Theory Model 10:603–623. doi:10.1080/13647830600578506

Wronski CRM (1967) The size dependence of the melting point of small particles of tin. Br J Appl Phys 18:1731–1737. doi:10.1088/0508-3443/18/12/308

Yetter R (2008) http://www.neem.psu.edu/

Zhou Y, Karplus M, Ball KD, Berry RS (2002) The distance fluctuation criterion for melting: Comparison of square well and More potential modes for clusters and homo polymers. J Chem Phys 116:2323–2329. doi:10.1063/1.1426419

Zou Y, Chen L (2005) Pressure dependence of the melting temperature of aluminum. Phys Stat Sol (b) 242:2412–2416